

# Thioether-Based Fluorescent Covalent Organic Framework for Selective Detection and Facile Removal of Mercury(II)

San-Yuan Ding,<sup>†</sup> Ming Dong,<sup>†</sup> Ya-Wen Wang,<sup>†</sup> Yan-Tao Chen,<sup>†</sup> Huai-Zhen Wang,<sup>†</sup> Cheng-Yong Su,<sup>‡</sup> and Wei Wang<sup>\*,†,§</sup>

<sup>†</sup>State Key Laboratory of Applied Organic Chemistry, College of Chemistry and Chemical Engineering, Lanzhou University, Lanzhou, Gansu 730000, China

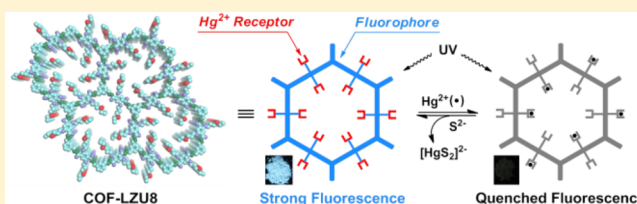
<sup>‡</sup>School of Chemistry and Chemical Engineering, Sun Yat-Sen University, Guangzhou 510275, China

<sup>§</sup>Collaborative Innovation Center of Chemical Science and Engineering, Tianjin 300071, China

## Supporting Information

**ABSTRACT:** Heavy metal ions are highly toxic and widely spread as environmental pollutants. New strategies are being developed to simultaneously detect and remove these toxic ions. Herein, we take the intrinsic advantage of covalent organic frameworks (COFs) and develop fluorescent COFs for sensing applications. As a proof-of-concept, a thioether-functionalized COF material, COF-LZU8, was “bottom-up” integrated with multifunctionality for the selective detection

and facile removal of mercury(II): the  $\pi$ -conjugated framework as the signal transducer, the evenly and densely distributed thioether groups as the  $\text{Hg}^{2+}$  receptor, the regular pores facilitating the real-time detection and mass transfer, together with the robust COF structure for recycle use. The excellent sensing performance of COF-LZU8 was achieved in terms of high sensitivity, excellent selectivity, easy visibility, and real-time response. Meanwhile, the efficient removal of  $\text{Hg}^{2+}$  from water and the recycling of COF-LZU8 offers the possibility for practical applications. In addition, X-ray photoelectron spectroscopy and solid-state NMR investigations verified the strong and selective interaction between  $\text{Hg}^{2+}$  and the thioether groups of COF-LZU8. This research not only demonstrates the utilization of fluorescent COFs for both sensing and removal of metal ions but also highlights the facile construction of functionalized COFs for environmental applications.



## INTRODUCTION

Because of the high toxicity and bioaccumulation, heavy metal ions released into the environment can lead to a wide range of severe diseases.<sup>1</sup> Considerable efforts<sup>2</sup> are accordingly being made to develop new methodologies for effective detection and removal of these toxic ions. For example, many types of small molecules have been designed as fluorescent sensors for selective and sensitive detection of the metal ions.<sup>3</sup> On the other hand, various absorbents, such as porous silicas,<sup>4</sup> hydrogels,<sup>4b,5</sup> nanoparticles,<sup>6</sup> and metal–organic frameworks (MOFs),<sup>7</sup> are being tested for the possible removal of the toxic ions. However, most of the developed methods can only perform either the detection or the removal task separately, which limits their practical applications.

Covalent organic frameworks (COFs) are a new type of crystalline porous materials purely constructed with organic building blocks.<sup>8</sup> Characteristics of tunable functionality, regular pore structure, and high surface area, many COFs have recently been constructed with different covalent linkages.<sup>9</sup> However, potential applications (such as for gas storage,<sup>10</sup> optoelectricity,<sup>11</sup> catalysis,<sup>12</sup> and sensing<sup>9g,1</sup>) are still at the very early stages of fundamental research. We envisioned that the functional COFs could work as the new candidates for both detection and removal of metal ions. First, the extended  $\pi$ -

conjugation framework can act as an excellent signal transducer by amplifying<sup>13</sup> the fluorescence change. In this regard, the rigid COF framework serves not only for the structural preservation but also for the signaling function. Second, both the “bottom-up” and “post-synthesis”<sup>14</sup> strategies can be applied to attach the specific ionophoric moieties to the fluorescent COF framework. Thus, the selective sensing toward diverse applications may be achieved. Third, the porous crystalline structure offers an excellent scaffold for hosting the metal ions for detection. Therefore, the easy access to the ionophoric sites within the regular channels is guaranteed for the real-time response. Finally, the enrichment of toxic metal ions inside the robust porous framework can be fulfilled as the prerequisite for further removal.

Herein, we report the first application of fluorescent COFs for detecting and removing the metal ions. As a proof-of-concept, a thioether-functionalized hydrazone-linked COF, COF-LZU8, was designed and applied for the selective sensing and effective removal of the toxic  $\text{Hg}^{2+}$  (Figure 1). The convenient “bottom-up” construction of COF-LZU8 was successfully achieved from the monomers 1 and 2 under

Received: October 14, 2015

Published: February 15, 2016

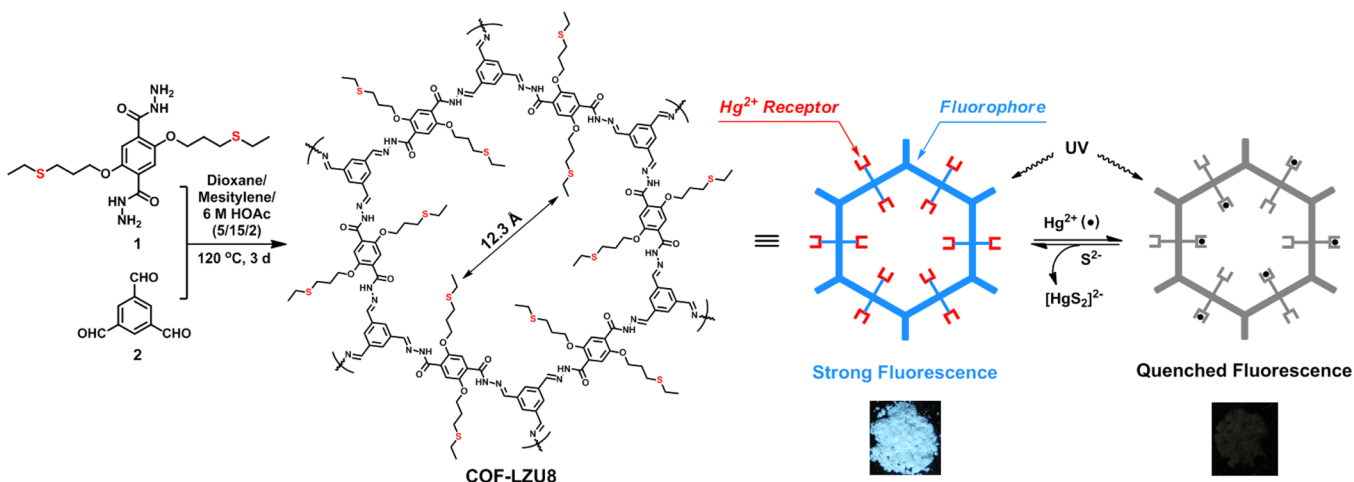
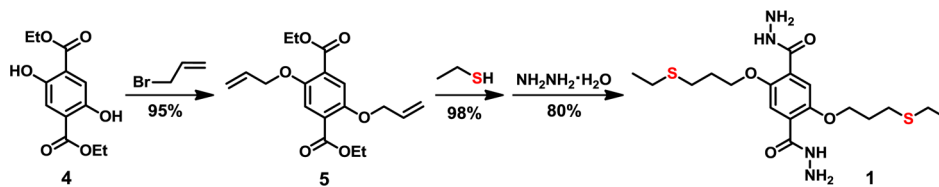


**Figure 1.** Synthesis of COF-LZU8 via the co-condensation of **1** and **2** under solvothermal conditions (see Supporting Information for details). For clarity, the extended COF-LZU8 structure is not shown. With the  $\pi$ -conjugated framework as the fluorophore and the thioether groups as the  $\text{Hg}^{2+}$  receptor, the synthesized COF-LZU8 was applied for both detection and removal of  $\text{Hg}^{2+}$  (see the main text). COF-LZU8 exhibited strong fluorescence upon excitation at 390 nm. Upon the addition of  $\text{Hg}^{2+}$ , the fluorescence of COF-LZU8 was effectively quenched. Photographs of COF-LZU8 under a UV lamp ( $\lambda_{\text{ex}} = 365 \text{ nm}$ ) visualize the significant change in the fluorescence emission before (left) and after (right) the adsorption of  $\text{Hg}^{2+}$ .

### Scheme 1. Facile Three-Step Synthesis of the Thioether Monomer **1** from Cheap and Commercially Available Compound **4**<sup>a</sup>



<sup>a</sup>The total yield from **4** to **1** is 74%. See Supporting Information for the synthetic details.

solvothermal conditions. In significant contrast from **1** and **2**, COF-LZU8 showed strong fluorescence both in the solid state and upon dispersion in solution. Importantly, the real-time fluorescence response did show efficient quenching of COF-LZU8 upon the addition of  $\text{Hg}^{2+}$ , together with its color change under a portable UV lamp. Excellent sensitivity and selectivity toward the  $\text{Hg}^{2+}$  detection were verified in the presence of other competitive cations. The removal ability of COF-LZU8 was further elucidated by the effective separation of  $\text{Hg}^{2+}$  from water. Both detection and removal of  $\text{Hg}^{2+}$  could be easily realized in the recycling experiments. In addition, X-ray photoelectron spectroscopy (XPS) and solid-state NMR spectroscopic analysis revealed the strong and selective interaction between  $\text{Hg}^{2+}$  and the sulfur atoms of COF-LZU8.

## RESULTS AND DISCUSSION

### Designed Synthesis and Structural Characterization.

As shown in Figure 1, the thioether-based hydrazone-linked COF material, COF-LZU8, was “bottom-up” constructed from the simple monomers **1** and **2** under solvothermal conditions. The synthetic conditions are quite mild, and COF-LZU8 could be reproducibly prepared (see Supporting Information for details). Our approach not only built the rigid and extended  $\pi$ -conjugation framework as the fluorophore (signal transducer) but also embedded the evenly and densely distributed thioether side chains as the ionophore (cation receptor). These unique characteristics together with the regular porous structure are expected to be beneficial for the performance in selective detection and facile removal of  $\text{Hg}^{2+}$ . In addition, with the total

yield of 74%, the key thioether monomer **1** was easily synthesized in three steps from the cheap and commercially available compound **4** (Scheme 1). As a result, COF-LZU8 can be readily prepared on a large scale for potential practical use.<sup>15</sup>

The crystalline structure of COF-LZU8 was determined by powder X-ray diffraction (PXRD) analysis with  $\text{Cu K}\alpha$  radiation. The experimental PXRD pattern (Figure 2, black) shows the diffraction peaks with  $d$  spacings of 25.30, 12.62, 9.60, 7.23, and 3.32 Å, corresponding to the 100, 200, 210, 220, and 001 reflections, respectively. The lattice modeling and Pawley refinement (Materials Studio, version 6.0) gave optimized parameters of  $a = b = 29.030 (\pm 0.446) \text{ \AA}$  and  $c = 3.667 (\pm 0.057) \text{ \AA}$  for the unit cell with the space group of  $P3$ . After the geometrical energy minimization, the refined PXRD pattern (Figure 2, orange) matches well with the experimental profile. Comparison of the observed and the simulated PXRD patterns (Figures S12 and S13) suggested the preferable structure as the eclipsed arrangement (Figure 2). Similar to the 2D cyclotricatechylene<sup>16</sup> and cyclotrimeratrylene<sup>17</sup> COFs, COF-LZU8 possesses a contorted structure (Figure 2, side view) with an interlayer distance of  $\sim 3.7 \text{ \AA}$ .

Identification of the eclipsed structure for COF-LZU8 was further supported by the pore size distribution analysis. Nitrogen adsorption–desorption experiment at 77 K (Figure 3) showed a type-I  $\text{N}_2$  adsorption isotherm, which is characteristic for a microporous structure. A slight offset may exist between the adjacent layers of COF-LZU8, which results in pore constrictions.<sup>11h</sup> The hysteresis in the desorption curve should be attributed to  $\text{N}_2$  trapped in these pore constrictions.

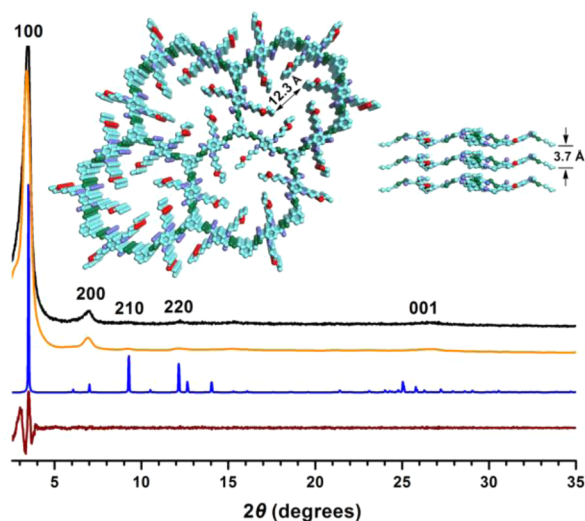


**Figure 2.** Experimental (black), Pawley refined (orange), and predicted (blue) PXRD patterns of COF-LZU8. The difference plot between the observed and the refined PXRD patterns is presented in brown. Inset: Eclipsed structure proposed for COF-LZU8. C, sky blue; N, green; O, purple; S, red. H atoms are omitted for clarity.

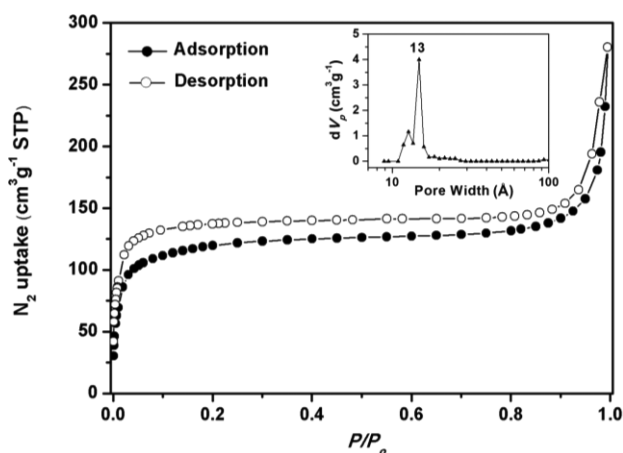


**Figure 3.** N<sub>2</sub> adsorption and desorption isotherms of COF-LZU8. Inset: Pore size distribution (with an average pore width of ~13 Å) of COF-LZU8 calculated by NLDFT.

The Brunauer–Emmett–Teller (BET) surface area of COF-LZU8 was calculated as 454 m<sup>2</sup> g<sup>-1</sup>, and the total pore volume was 0.36 cm<sup>3</sup> g<sup>-1</sup> ( $P/P_0 = 0.99$ ), which matches that (0.39 cm<sup>3</sup> g<sup>-1</sup>) calculated by PLATON.<sup>18</sup> The nonlocal density functional theory (NLDFT) gave rise to a narrow pore size distribution with an average pore width of ~13 Å (Figure 3, inset), which agrees well with the calculated value of 12.3 Å based on the eclipsed structure (Figure 2).

With the robust hydrazone linkage in its structure, COF-LZU8 is insoluble and stable in common organic solvents, such as *N,N*-dimethylformamide (DMF), tetrahydrofuran (THF), dimethylsulfoxide (DMSO), acetone, and trichloromethane. Importantly, COF-LZU8 is also insoluble and very stable in water; its crystalline structure can be preserved in aqueous solution at pH 3–13 (Figure S16). Thermogravimetric analysis (TGA) indicates that COF-LZU8 is thermally stable up to 310 °C (Figure S21). The scanning electron microscopy (SEM) images showed that COF-LZU8 possessed the uniform sphere-like morphology with an average particle size of ~250 nm

(Figure S22). A characteristic vibrational band appeared at 1621 cm<sup>-1</sup> in the FT-IR spectrum of COF-LZU8 (Figure S1), indicating the successful condensation of 1 and 2 via the formation of –C=N– bonds.

**Fluorescence Property.** The luminescence properties of COF-LZU8 were studied by UV/vis and fluorescence spectroscopy. COF-LZU8 displayed a UV absorption band at ~390 nm in the solid state (Figure S3). Due to the extended  $\pi$ -conjugation in the COF-LZU8 framework, its absorption band is bathochromic (Figure S3) from those of the monomers (1 and 2) and the model compound 3 (as a small-molecule counterpart of COF-LZU8, structure shown in Figure 4). The

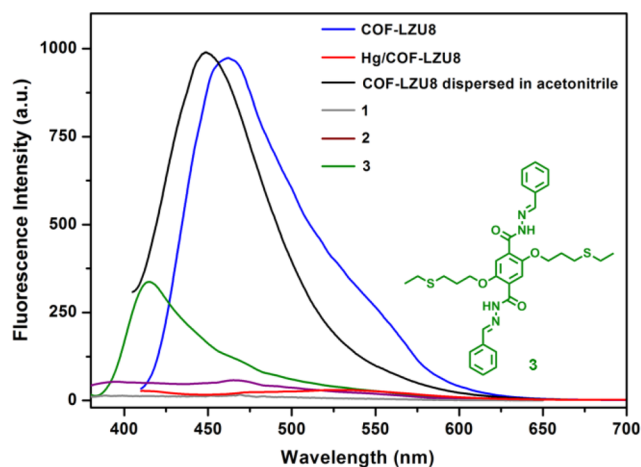


**Figure 4.** Fluorescence spectra of 1 (gray), 2 (purple), model compound 3 (green), COF-LZU8 (blue), and Hg/COF-LZU8 (red) in the solid state. Meanwhile, insoluble COF-LZU8 can be dispersed in solvents, and the fluorescence spectrum of COF-LZU8 dispersed in acetonitrile is shown (black).

fluorescence spectrum of COF-LZU8 in the solid state (Figure 4, blue) exhibits a maximum emission band at 460 nm with an absolute quantum yield ( $\Phi_F$ ) of 3.5% upon excitation at 390 nm. On the contrary, the corresponding monomers 1 and 2 display essentially no fluorescence in the solid state upon excitation at 390 or 366 nm (Figure 4, gray and purple). Meanwhile, the model compound 3 only shows a weak emission band at 415 nm (Figure 4, green) and a low quantum yield ( $\Phi_F = 0.8\%$ ) upon excitation at 366 nm. The significant difference in the luminescence properties between COF-LZU8 and its structural monomers (1, 2, or 3) should be attributed to the extended  $\pi$ -conjugation framework in COF-LZU8. This difference highlights the uniqueness of using  $\pi$ -conjugated COF materials for fluorescent applications. Moreover, COF-LZU8 is readily dispersed in acetonitrile and other organic solvents (such as THF, DMF, and ethanol), exhibiting a strong emission peak at ~450 nm upon excitation at 390 nm (Figure 4, black, and Figure S6). Therefore, COF-LZU8 keeps its high fluorescence in solvents as well, which is the prerequisite for the real-time detection of Hg<sup>2+</sup> in solution.

It is worth mentioning that the 2D imine-linked COF-LZU1<sup>12a</sup> shows negligible fluorescence in the solid state (Figure S4). The fully planar structure of COF-LZU1 may lead to the “aggregation-caused quenching (ACQ)”, which normally turns off the light emission.<sup>19</sup> As shown in Figure 2, the contorted structure could efficiently avoid the ACQ effect<sup>20</sup> and, therefore, renders COF-LZU8 highly fluorescent. Meanwhile, the strong fluorescence of COF-LZU8 might be contributed

partially from the thioether groups; a similar case has been found for the thioether-functionalized MOF.<sup>21</sup>

**Detection and Removal of Hg<sup>2+</sup>.** The finding of strong fluorescence for COF-LZU8 intrigued us to further explore its sensing applications. Mercury has been recognized as one of the most toxic heavy metals, leading to the dysfunction of organs and the central nervous system.<sup>22</sup> New probes are highly desired to monitor and remove Hg<sup>2+</sup> in environmental and biological systems.<sup>22a,23</sup> Due to the distinct  $\pi$ -donor character and specific affinity, sulfur groups are the privileged ionophoric receptor for Hg<sup>2+</sup>. Aiming to reach the high sensitivity, unique selectivity, and simple handling, fluorescent organosulfur compounds have been tested as the Hg<sup>2+</sup> chemosensor.<sup>24</sup> Accordingly, we applied the thioether-based fluorescent COF-LZU8 first for the possible detection and removal of Hg<sup>2+</sup>.

The sensitivity of COF-LZU8 toward the Hg<sup>2+</sup> detection was evaluated via the real-time fluorescence response. For this purpose, the stock solution of Hg(ClO<sub>4</sub>)<sub>2</sub> was gradually added to the suspension of COF-LZU8 in acetonitrile, and the corresponding fluorescence spectra were measured immediately. As shown in Figure 5, upon the addition of Hg<sup>2+</sup>, the

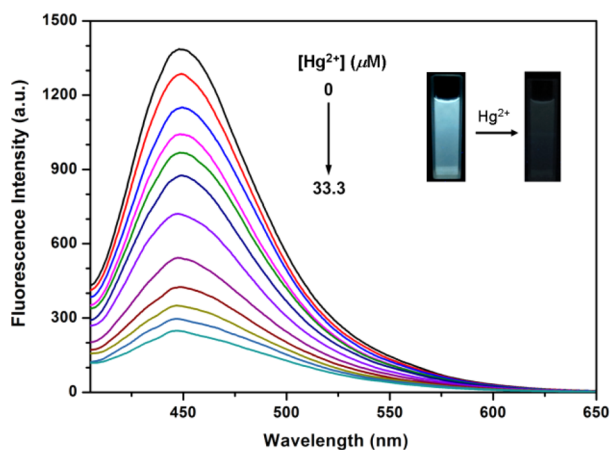


**Figure 5.** Fluorescence titration of COF-LZU8 dispersed in acetonitrile upon the gradual addition of Hg<sup>2+</sup> ( $\lambda_{\text{ex}} = 390$  nm). Inset: Photographs of fluorescence emission change (under a UV lamp with  $\lambda_{\text{ex}} = 365$  nm) of COF-LZU8 in acetonitrile upon the addition of Hg<sup>2+</sup>.

quenching of the fluorescence emission of COF-LZU8, accompanied by its color change under a portable UV lamp (with  $\lambda_{\text{ex}} = 365$  nm), was clearly observed. Eighty-three percent of the total fluorescence intensity of COF-LZU8 could be quenched upon the addition of only 33.3  $\mu\text{M}$  of Hg<sup>2+</sup>. In contrast, another hydrazone-linked COF-42 with the ethoxy groups as the side chains<sup>9i</sup> exhibited an extremely weak response to Hg<sup>2+</sup> (Figure S8). This discrepancy suggested that the quenched fluorescence in Figure 5 should originate from the interaction between the thioether groups of COF-LZU8 and Hg<sup>2+</sup>. The detection limit for Hg<sup>2+</sup> was determined as 25.0 ppb (Figure S11). This value represents an excellent sensitivity<sup>22a</sup> toward the Hg<sup>2+</sup> detection, which is superior to many thioether-functionalized chemosensors.<sup>24g,l</sup>

We further measured the Hg<sup>2+</sup> contents in the COF-LZU8 samples by inductively coupled plasma (ICP) analysis. The ICP results indicate that COF-LZU8 with 11.6% of the Hg<sup>2+</sup> content (corresponding to 1.6 Hg atoms per unit cell) resulted in 80% of the fluorescence quenching (Figures S9 and S10).

Given that one unit cell contains six thioether groups, unsaturated coordination of these thioether groups with Hg<sup>2+</sup> can lead to efficient fluorescence quenching. This result indicates clearly the amplified fluorescence response for COF-LZU8 in the detection of Hg<sup>2+</sup>.

The selectivity of COF-LZU8 toward the Hg<sup>2+</sup> detection was then investigated by testing the fluorescence change in the presence of other metal ions. As shown in Figure 6a, among all

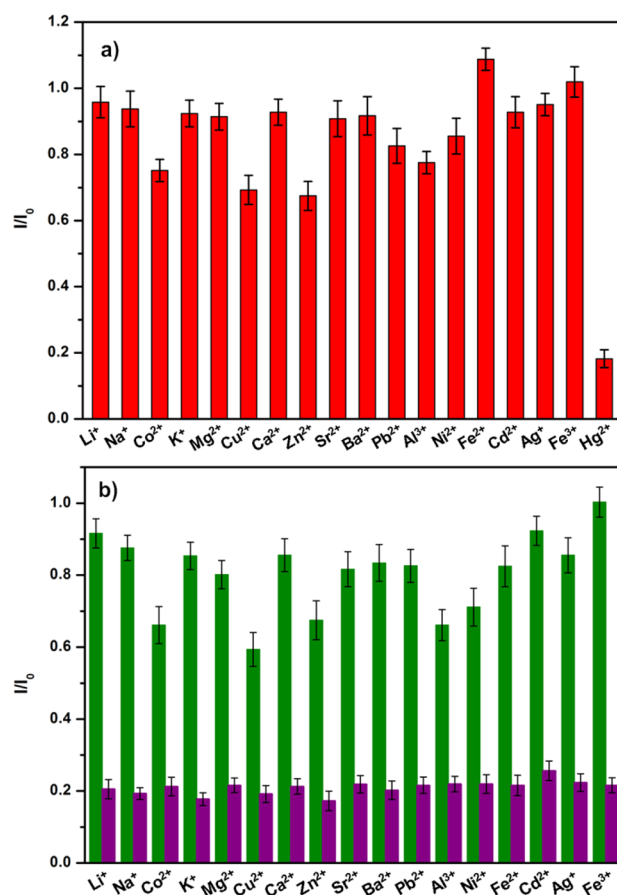


**Figure 6.** Selectivity of COF-LZU8 toward Hg<sup>2+</sup> detection: (a) fluorescence response of COF-LZU8 in the presence of different metal ions (33.3  $\mu\text{M}$ ) in acetonitrile ( $\lambda_{\text{ex}} = 390$  nm) and (b) competition experiments. The green bars in (b) represent the emission intensity of COF-LZU8 in the presence of the competition ions (2.0 equiv), and the purple bars represent the emission intensity upon the addition of Hg<sup>2+</sup> (1.0 equiv) to the above solutions. The error bars represent the standard deviation of three independent measurements.

the metal ions examined, only Hg<sup>2+</sup> caused the significant fluorescence quenching of COF-LZU8. To verify the selectivity of COF-LZU8 for the practical detection of Hg<sup>2+</sup>, the competition experiments were further conducted by addition of Hg<sup>2+</sup> (1.0 equiv) to the acetonitrile solution of the competitive metal ions (2.0 equiv). As shown in Figure 6b, neither of the competitive metal ions showed an appreciable influence on the Hg<sup>2+</sup> detection. These results further identified that COF-LZU8 exhibits a satisfactory selectivity toward Hg<sup>2+</sup> detection.

The sensing methods developed so far can hardly perform the double duties of detection and removal of metal ions, especially in aqueous solution. We found that COF-LZU8 worked well in aqueous solution. Similar to the cases in organic

solvents, COF-LZU8 showed high fluorescence in water and efficient fluorescence quenching upon the addition of  $\text{Hg}^{2+}$  (Figure S6). In order to assess the  $\text{Hg}^{2+}$  uptake capacity in water for potential practical applications, we treated 20 mg of COF-LZU8 with an aqueous solution of  $\text{Hg}(\text{ClO}_4)_2$  (0.1 M, 2.2 mL) followed by drying. Similar to those found in acetonitrile (Figure 5) and in water (Figure S6), the obtained  $\text{Hg}/\text{COF-LZU8}$  powders displayed essentially no fluorescence upon excitation at 390 nm (Figure 4, red). The ICP analysis identified a high Hg content of 23.6 wt %, corresponding to  $\sim 2.5$  Hg atoms per unit cell. To further illustrate the effective removal of  $\text{Hg}^{2+}$  from water, COF-LZU8 (5 mg) was suspended in a dilute aqueous solution of  $\text{Hg}(\text{ClO}_4)_2$  (10 ppm in 5.0 mL). After the suspension was stirred for 3 h, the concentration of the residual  $\text{Hg}^{2+}$  in water was less than 0.2 ppm, indicating that over 98% of  $\text{Hg}^{2+}$  could be effectively removed even in extremely dilute solutions. In comparison with the thioether-functionalized MOF,<sup>21</sup> COF-LZU8 shows even better capability for  $\text{Hg}^{2+}$  removal. This may be attributed to the 2D eclipsed structure of COF-LZU8: the straight channel with a diameter of  $\sim 13$  Å facilitates the access between the  $\text{Hg}^{2+}$  and the S atoms of COF-LZU8.

Unlike in organic solvents, the uniform dispersion of COF-LZU8 in water is, however, not easy to maintain. This phenomenon prevented us from obtaining the quantitative data for the systematic assessment of its sensing performance in water. Nevertheless, this would not hinder the potential use of COF-LZU8 at all for both detection (Figure S6) and removal of  $\text{Hg}^{2+}$  in water, especially when the advantages of COF-LZU8 (such as easy preparation, low cost, excellent stability, and insensitivity to pH values) are taken into account together with its excellent capability for removing the  $\text{Hg}^{2+}$  (vide infra).

On the basis of the excellent  $\text{Hg}^{2+}$  uptake capacity, we further explored the recycle use of COF-LZU8. Upon the simple treatment with 10 equiv of aqueous  $\text{Na}_2\text{S}$  solution to exchange the adsorbed  $\text{Hg}^{2+}$  out,<sup>25</sup> the fluorescence of COF-LZU8 could be easily recovered (see Supporting Information for details). As shown in Figure 7, this  $\text{Hg}^{2+}$  adsorption–desorption cycle

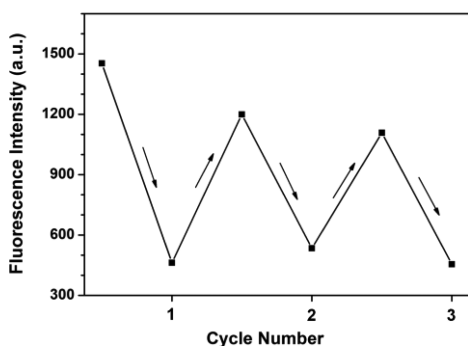


**Figure 7.** Recycle use of COF-LZU8 for selective detection and facile removal of the toxic  $\text{Hg}^{2+}$ . Upon treatment in aqueous  $\text{Na}_2\text{S}$  solution, COF-LZU8 was easily recovered and could be repeatedly used.

could be repeated at least three times without significant loss of the sensitivity and responsiveness of COF-LZU8. Meanwhile, the crystalline structure of COF-LZU8 was well preserved after the  $\text{Hg}^{2+}$  exchange (Figure S15).

**Interaction between Thioether and  $\text{Hg}^{2+}$ .** To gain further insights into the structure–property performance relationship for COF-LZU8 in the selective detection and effective removal of  $\text{Hg}^{2+}$ , we applied XPS to evaluate the

interaction between  $\text{Hg}^{2+}$  and the thioether groups. As shown in Figure 8a, the binding energy (BE) of S  $2p_{3/2}$  in COF-LZU8

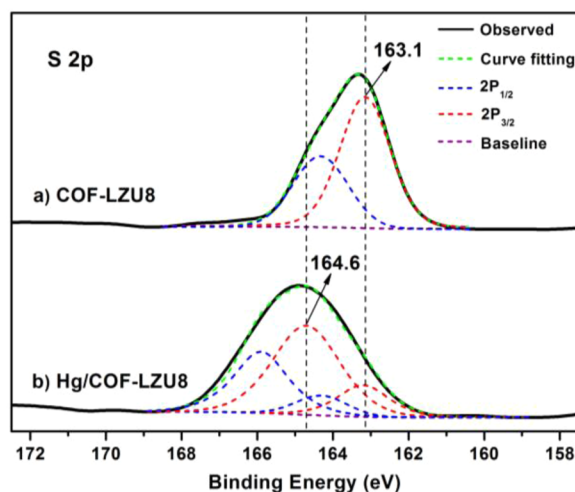


**Figure 8.** XPS spectra of COF-LZU8 (a) and  $\text{Hg}/\text{COF-LZU8}$  (b). The experimental spectra are shown as solid curves, and the fitting data are shown in dotted curves.

was measured as 163.1 eV, which is in agreement with that generally found<sup>26</sup> for organosulfur compounds. On the contrary, upon the adsorption of  $\text{Hg}^{2+}$ , the BE of S  $2p_{3/2}$  in  $\text{Hg}/\text{COF-LZU8}$  was mostly shifted to 164.6 eV (Figure 8b). The positive shift by 1.5 eV evidenced the interaction between S and  $\text{Hg}^{2+}$  in  $\text{Hg}/\text{COF-LZU8}$ : electrons were further donated to  $\text{Hg}^{2+}$ , which makes the S atoms electron-deficient.<sup>26</sup>

Solid-state  $^{13}\text{C}$  cross-polarization magic-angle spinning (CP/MAS) NMR spectroscopy further provided the overwhelming evidence for the strong and selective interaction between  $\text{Hg}^{2+}$  and the S atoms. The  $^{13}\text{C}$  CP/MAS NMR spectrum of COF-LZU8 is shown in Figure 9a, and the signal assignments are depicted on the top. Upon the adsorption of  $\text{Hg}^{2+}$ , the  $^{13}\text{C}$  NMR signal at 28 ppm, which is ascribed to the methylene carbons adjacent to the S atoms in COF-LZU8, was downfield<sup>4b</sup> shifted to 35 ppm (Figure 9b), while other signals were unchanged. This result identified the strong interaction between S and  $\text{Hg}^{2+}$  in  $\text{Hg}/\text{COF-LZU8}$ . Meanwhile, after the treatment of  $\text{Hg}/\text{COF-LZU8}$  with  $\text{Na}_2\text{S}$ , the  $^{13}\text{C}$  CP/MAS NMR spectrum recorded thereafter (Figure 9c) closely resembles that of fresh COF-LZU8. This result verified the recycle use of COF-LZU8 for facile removal of  $\text{Hg}^{2+}$ . Moreover, in order to further confirm the selective interaction with  $\text{Hg}^{2+}$ , the fresh COF-LZU8 was treated with  $\text{Cd}(\text{ClO}_4)_2$ . The obtained  $\text{Cd}/\text{COF-LZU8}$  sample (Figure 9d) gave almost the identical  $^{13}\text{C}$  CP/MAS NMR spectrum as COF-LZU8, indicating that no interaction existed between  $\text{Cd}^{2+}$  and COF-LZU8.

Therefore, the selective detection and effective removal of  $\text{Hg}^{2+}$  for COF-LZU8 stems indeed from the strong and selective interaction between  $\text{Hg}^{2+}$  and the S atoms. It is well-known that most of the  $\text{Hg}^{2+}$  sensors are “turn off” sensors because  $\text{Hg}^{2+}$  possesses intrinsically a chelation-enhanced quenching effect.<sup>27</sup> In the case of COF-LZU8, it is very likely that the  $\text{Hg}^{2+}$  first bound to the S atoms and the electrons were then transferred from the  $\pi$ -conjugation framework to the unoccupied orbitals of  $\text{Hg}^{2+}$ , resulting in the significant fluorescence quenching. Other metal ions, such as  $\text{Cd}^{2+}$ ,

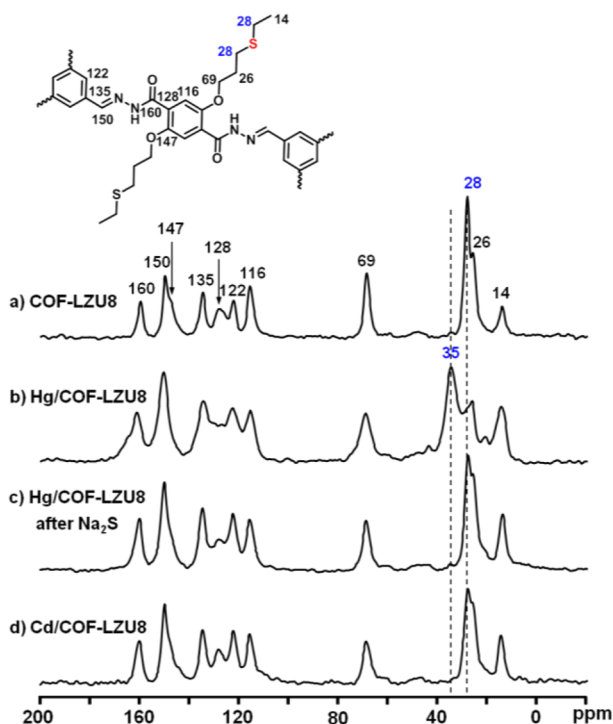


**Figure 9.**  $^{13}\text{C}$  CP/MAS NMR spectra of COF-LZU8 (a), Hg/COF-LZU8 (b), and Hg/COF-LZU8 after the treatment with  $\text{Na}_2\text{S}$  (c). The signal at 28 ppm of COF-LZU8 (a) was downfield shifted to 35 ppm in Hg/COF-LZU8 (b), which verified the strong interaction between  $\text{Hg}^{2+}$  and S. On the contrary, the  $^{13}\text{C}$  CP/MAS NMR spectrum of Cd/COF-LZU8 (d) is almost identical to that of COF-LZU8 (a), indicating that COF-LZU8 cannot bind with  $\text{Cd}^{2+}$  strongly.

could not bind with the S atoms effectively, and therefore, their effects on the fluorescence are negligible.

## CONCLUSION

In conclusion, we demonstrate in this contribution that fluorescent COFs can be designed and synthesized for efficient detection and removal of metal ions. Possessing the unique nature of the extended  $\pi$ -conjugation framework, tunable functionality, and regular pore structure, COF materials are new and ideal candidates with intrinsic “all-in-one” sensing functionalities. As an example toward the potential practical application, a thioether-based hydrazone-linked COF-LZU8 was rationally designed and easily constructed for highly sensitive detection and effective removal of  $\text{Hg}^{2+}$ . Due to the high stability of the hydrazone linkages, together with the dense distribution of the thioether groups and the straight channels in COF-LZU8, the recycling of COF-LZU8 achieved the simultaneous detection and removal of the toxic  $\text{Hg}^{2+}$ .

This research not only explored the construction strategy of fluorescent COFs but also expanded the COF applications from gas storage/separation to cation sensing/adsorption/removal. In addition, by realizing the new application of hydrazone-linked COF, we paved the way to construct and utilize the structurally robust hydrazone COFs. The synthetic route in Scheme 1 should be applicable to synthesize diverse monomers for constructing functional hydrazone COFs with tunable pore size: the existence of alkenyl (or alkynyl) side chains in the key intermediate **5** makes many modifications possible. We expect that our effort will benefit future research

on employing fluorescent and hydrazone COFs for environmental and industrial applications.

## ASSOCIATED CONTENT

### Supporting Information

The Supporting Information is available free of charge on the ACS Publications website at DOI: 10.1021/jacs.5b10754.

Experimental procedures; FT-IR, UV/vis, and fluorescence spectra; SEM images, PXRD patterns, modeling details, and atomic coordinates;  $\text{N}_2$  adsorption and TGA traces; liquid NMR data (PDF)

## AUTHOR INFORMATION

### Corresponding Author

\*wang\_wei@lzu.edu.cn

### Notes

The authors declare no competing financial interest.

## ACKNOWLEDGMENTS

This work was supported by the National Natural Science Foundation for Distinguished Young Scholars of China (No. 21425206), the 973 Program of China (2012CB821701), and the Specialized Research Fund for the Doctoral Program of Higher Education (20120211130004). We thank Prof. Qi-Yu Zheng (Institute of Chemistry, The Chinese Academy of Sciences) and Prof. Wei Yu (Lanzhou University) for helpful discussion.

## REFERENCES

- Schwarzenbach, R. P.; Escher, B. I.; Fenner, K.; Hofstetter, T. B.; Johnson, C. A.; von Gunten, U.; Wehrli, B. *Science* **2006**, *313*, 1072.
- (a) You, L.; Zha, D.; Anslyn, E. V. *Chem. Rev.* **2015**, *115*, 7840. (b) Vendrell, M.; Zhai, D.; Er, J. C.; Chang, Y.-T. *Chem. Rev.* **2012**, *112*, 4391. (c) Kreno, L. E.; Leong, K.; Farha, O. K.; Allendorf, M.; Van Duyne, R. P.; Hupp, J. T. *Chem. Rev.* **2012**, *112*, 1105. (d) Jung, J. H.; Lee, J. H.; Shinkai, S. *Chem. Soc. Rev.* **2011**, *40*, 4464. (e) Dave, N.; Chan, M. Y.; Huang, P.-J. J.; Smith, B. D.; Liu, J. *J. Am. Chem. Soc.* **2010**, *132*, 12668.
- (a) Carter, K. P.; Young, A. M.; Palmer, A. E. *Chem. Rev.* **2014**, *114*, 4564. (b) Li, X.; Gao, X.; Shi, W.; Ma, H. *Chem. Rev.* **2014**, *114*, 590. (c) Kim, H. N.; Ren, W. X.; Kim, J. S.; Yoon, J. *Chem. Soc. Rev.* **2012**, *41*, 3210. (d) Du, J.; Hu, M.; Fan, J.; Peng, X. *Chem. Soc. Rev.* **2012**, *41*, 4511. (e) Quang, D. T.; Kim, J. S. *Chem. Rev.* **2010**, *110*, 6280.
- (a) Wu, Z.; Zhao, D. *Chem. Commun.* **2011**, *47*, 3332. (b) Feng, X.; Fryxell, G. E.; Wang, L.-Q.; Kim, A. Y.; Liu, J.; Kemner, K. M. *Science* **1997**, *276*, 923.
- (a) Esser-Kahn, A. P.; Iavarone, A. T.; Francis, M. B. *J. Am. Chem. Soc.* **2008**, *130*, 15820. (b) Oh, Y.; Morris, C. D.; Kanatzidis, M. G. *J. Am. Chem. Soc.* **2012**, *134*, 14604.
- Khajeh, M.; Laurent, S.; Dastafkan, K. *Chem. Rev.* **2013**, *113*, 7728.
- (a) Yee, K.-K.; Reimer, N.; Liu, J.; Cheng, S.-Y.; Yiu, S.-M.; Weber, J.; Stock, N.; Xu, Z. *J. Am. Chem. Soc.* **2013**, *135*, 7795. (b) Abney, C. W.; Gilhula, J. C.; Lu, K.; Lin, W. *Adv. Mater.* **2014**, *26*, 7993. (c) Fang, Q.-R.; Yuan, D.-Q.; Sculley, J.; Li, J.-R.; Han, Z.-B.; Zhou, H.-C. *Inorg. Chem.* **2010**, *49*, 11637.
- (a) Côté, A. P.; Benin, A. L.; Ockwig, N. W.; O’Keeffe, M.; Matzger, A. J.; Yaghi, O. M. *Science* **2005**, *310*, 1166. (b) Feng, X.; Ding, X.; Jiang, D. *Chem. Soc. Rev.* **2012**, *41*, 6010. (c) Ding, S.-Y.; Wang, W. *Chem. Soc. Rev.* **2013**, *42*, 548. (d) Colson, J. W.; Dichtel, W. R. *Nat. Chem.* **2013**, *5*, 453.
- For selected examples, see: (a) El-Kaderi, H. M.; Hunt, J. R.; Mendoza-Cortes, J. L.; Côté, A. P.; Taylor, R. E.; O’Keeffe, M.; Yaghi, O. M. *Science* **2007**, *316*, 268. (b) Tilford, R. W.; Gemmill, W. R.; zur

- Loye, H.-C.; Lavigne, J. J. *Chem. Mater.* **2006**, *18*, 5296. (c) Colson, J. W.; Woll, A. R.; Mukherjee, A.; Leventorf, M. P.; Spittler, E. L.; Shields, V. B.; Spencer, M. G.; Park, J.; Dichtel, W. R. *Science* **2011**, *332*, 228. (d) Uribe-Romo, F. J.; Hunt, J. R.; Furukawa, H.; Klock, C.; O'Keefe, M.; Yaghi, O. M. *J. Am. Chem. Soc.* **2009**, *131*, 4570. (e) Zhang, Y.-B.; Su, J.; Furukawa, H.; Yun, Y.; Gándara, F.; Duong, A.; Zou, X.; Yaghi, O. M. *J. Am. Chem. Soc.* **2013**, *135*, 16336. (f) Kandambeth, S.; Mallick, A.; Lukose, B.; Mane, M. V.; Heine, T.; Banerjee, R. *J. Am. Chem. Soc.* **2012**, *134*, 19524. (g) Das, G.; Biswal, B. P.; Kandambeth, S.; Venkatesh, V.; Kaur, G.; Addicoat, M.; Heine, T.; Verma, S.; Banerjee, R. *Chem. Sci.* **2015**, *6*, 3931. (h) Kuhn, P.; Antonietti, M.; Thomas, A. *Angew. Chem., Int. Ed.* **2008**, *47*, 3450. (i) Uribe-Romo, F. J.; Doonan, C. J.; Furukawa, H.; Oisaki, K.; Yaghi, O. M. *J. Am. Chem. Soc.* **2011**, *133*, 11478. (j) Jackson, K. T.; Reich, T. E.; El-Kaderi, H. M. *Chem. Commun.* **2012**, *48*, 8823. (k) Nagai, A.; Chen, X.; Feng, X.; Ding, X.; Guo, Z.; Jiang, D. *Angew. Chem., Int. Ed.* **2013**, *52*, 3770. (l) Dalapati, S.; Jin, S.; Gao, J.; Xu, Y.; Nagai, A.; Jiang, D. *J. Am. Chem. Soc.* **2013**, *135*, 17310. (m) Beaudoin, D.; Maris, T.; Wuest, J. D. *Nat. Chem.* **2013**, *5*, 830. (n) Zhou, T.-Y.; Xu, S.-Q.; Wen, Q.; Pang, Z.-F.; Zhao, X. *J. Am. Chem. Soc.* **2014**, *136*, 15885. (o) Zeng, Y.; Zou, R.; Luo, Z.; Zhang, H.; Yao, X.; Ma, X.; Zou, R.; Zhao, Y. *J. Am. Chem. Soc.* **2015**, *137*, 1020.
- (10) (a) Furukawa, H.; Yaghi, O. M. *J. Am. Chem. Soc.* **2009**, *131*, 8875. (b) Doonan, C. J.; Tranchemontagne, D. J.; Glover, T. G.; Hunt, J. R.; Yaghi, O. M. *Nat. Chem.* **2010**, *2*, 235.
- (11) For selected examples, see: (a) Wan, S.; Guo, J.; Kim, J.; Ihee, H.; Jiang, D. *Angew. Chem., Int. Ed.* **2008**, *47*, 8826. (b) Wan, S.; Guo, J.; Kim, J.; Ihee, H.; Jiang, D. *Angew. Chem., Int. Ed.* **2009**, *48*, 5439. (c) Spittler, E. L.; Dichtel, W. R. *Nat. Chem.* **2010**, *2*, 672. (d) Wan, S.; Gandara, F.; Asano, A.; Furukawa, H.; Saeki, A.; Dey, S. K.; Liao, L.; Ambrogio, M. W.; Botros, Y. Y.; Duan, X.; Seki, S.; Stoddart, J. F.; Yaghi, O. M. *Chem. Mater.* **2011**, *23*, 4094. (e) DeBlase, C. R.; Silberstein, K. E.; Truong, T.-T.; Abruña, H. D.; Dichtel, W. R. *J. Am. Chem. Soc.* **2013**, *135*, 16821. (f) Dogru, M.; Handloser, M.; Auras, F.; Kunz, T.; Medina, D.; Hartschuh, A.; Knochel, P.; Bein, T. *Angew. Chem., Int. Ed.* **2013**, *52*, 2920. (g) Bertrand, G. H. V.; Michaelis, V. K.; Ong, T.-C.; Griffin, R. G.; Dincă, M. *Proc. Natl. Acad. Sci. U. S. A.* **2013**, *110*, 4923. (h) Spittler, E. L.; Koo, B. T.; Novotney, J. L.; Colson, J. W.; Uribe-Romo, F. J.; Gutierrez, G. D.; Clancy, P.; Dichtel, W. R. *J. Am. Chem. Soc.* **2011**, *133*, 19416.
- (12) (a) Ding, S.-Y.; Gao, J.; Wang, Q.; Zhang, Y.; Song, W.-G.; Su, C.-Y.; Wang, W. *J. Am. Chem. Soc.* **2011**, *133*, 19816. (b) Stegbauer, L.; Schwinghammer, K.; Lotsch, B. V. *Chem. Sci.* **2014**, *5*, 2789. (c) Fang, Q.; Gu, S.; Zheng, J.; Zhuang, Z.; Qiu, S.; Yan, Y. *Angew. Chem., Int. Ed.* **2014**, *53*, 2878.
- (13) (a) Thomas, S. W.; Joly, G. D.; Swager, T. M. *Chem. Rev.* **2007**, *107*, 1339. (b) Toal, S. J.; Trogler, W. C. *J. Mater. Chem.* **2006**, *16*, 2871.
- (14) (a) Nagai, A.; Guo, Z.; Feng, X.; Jin, S.; Chen, X.; Ding, X.; Jiang, D. *Nat. Commun.* **2011**, *2*, 536. (b) Bunck, D. N.; Dichtel, W. R. *Chem. Commun.* **2013**, *49*, 2457.
- (15) Chinese Patent Application No. 201310693080.9, 2013.
- (16) Yu, J.-T.; Chen, Z.; Sun, J.; Huang, Z.-T.; Zheng, Q.-Y. *J. Mater. Chem.* **2012**, *22*, 5369.
- (17) Song, J.-R.; Sun, J.; Liu, J.; Huang, Z.-T.; Zheng, Q.-Y. *Chem. Commun.* **2014**, *50*, 788.
- (18) Spek, A. L. *J. Appl. Crystallogr.* **2003**, *36*, 7.
- (19) Birks, J. B. *Photophysics of Aromatic Molecules*; Wiley: London, 1970.
- (20) Hong, Y.; Lam, J. W. Y.; Tang, B. Z. *Chem. Soc. Rev.* **2011**, *40*, 5361.
- (21) He, J.; Yee, K.-K.; Xu, Z.; Zeller, M.; Hunter, A. D.; Chui, S. S.-Y.; Che, C.-M. *Chem. Mater.* **2011**, *23*, 2940.
- (22) (a) Nolan, E. M.; Lippard, S. J. *Chem. Rev.* **2008**, *108*, 3443. (b) Quang, D. T.; Kim, J. S. *Chem. Rev.* **2010**, *110*, 6280.
- (23) For selected examples, see: (a) Climent, E.; Marcos, M. D.; Martínez-Mañez, R.; Sancenón, F.; Soto, J.; Rurack, K.; Amorós, P. *Angew. Chem., Int. Ed.* **2009**, *48*, 8519. (b) Ye, B.-C.; Yin, B.-C. *Angew. Chem., Int. Ed.* **2008**, *47*, 8386. (c) Ros-Lis, J. V.; Casasús, R.; Comes, M.; Coll, C.; Marcos, M. D.; Martínez-Mañez, R.; Sancenón, F.; Soto, J.; Amorós, P.; Haskouri, J. E.; Garró, N.; Rurack, K. *Chem. - Eur. J.* **2008**, *14*, 8267. (d) Li, J.; Wu, Y.; Song, F.; Wei, G.; Cheng, Y.; Zhu, C. *J. Mater. Chem.* **2012**, *22*, 478.
- (24) For selected examples, see: (a) Nolan, E. M.; Lippard, S. J. *J. Am. Chem. Soc.* **2003**, *125*, 14270. (b) Yoon, S.; Albers, A. E.; Wong, A. P.; Chang, C. J. *J. Am. Chem. Soc.* **2005**, *127*, 16030. (c) Coronado, E.; Galán-Mascarós, J. R.; Martí-Gastaldo, C.; Palomares, E.; Durrant, J. R.; Vilar, R.; Gratzel, M.; Nazeeruddin, M. K. *J. Am. Chem. Soc.* **2005**, *127*, 12351. (d) Zhao, Y.; Zhong, Z. *J. Am. Chem. Soc.* **2006**, *128*, 9988. (e) Huang, J.; Xu, Y.; Qian, X. *J. Org. Chem.* **2009**, *74*, 2167. (f) Yang, Y.-K.; Yook, K.-J.; Tae, J. *J. Am. Chem. Soc.* **2005**, *127*, 16760. (g) Descalzo, A. B.; Martínez-Mañez, R.; Radeaglia, R.; Rurack, K.; Soto, J. *J. Am. Chem. Soc.* **2003**, *125*, 3418. (h) Rurack, K.; Kollmannsberger, M.; Resch-Genger, U.; Daub, J. *J. Am. Chem. Soc.* **2000**, *122*, 968. (i) Chen, X.; Nam, S.-W.; Jou, M. J.; Kim, Y.; Kim, S.-J.; Park, S.; Yoon, J. *Org. Lett.* **2008**, *10*, 5235. (j) Dong, M.; Wang, Y.-W.; Peng, Y. *Org. Lett.* **2010**, *12*, 5310. (k) Wu, J.-S.; Hwang, I.-C.; Kim, K. S.; Kim, J. S. *Org. Lett.* **2007**, *9*, 907. (l) Kim, S. H.; Song, K. C.; Ahn, S.; Kang, Y. S.; Chang, S.-K. *Tetrahedron Lett.* **2006**, *47*, 497. (m) Lee, M. H.; Lee, S. W.; Kim, S. H.; Kang, C.; Kim, J. S. *Org. Lett.* **2009**, *11*, 2101. (n) Li, M.-J.; Chu, B. W.-K.; Zhu, N.; Yam, V. W.-W. *Inorg. Chem.* **2007**, *46*, 720.
- (25) (a) Zhou, Y.; Zhu, C.-Y.; Gao, X.-S.; You, X.-Y.; Yao, C. *Org. Lett.* **2010**, *12*, 2566. (b) Wu, D.; Huang, W.; Lin, Z.; Duan, C.; He, C.; Wu, S.; Wang, D. *Inorg. Chem.* **2008**, *47*, 7190. (c) Findlay, D. M.; McLean, R. A. N. *Environ. Sci. Technol.* **1981**, *15*, 1388. (d) Armstrong, R. D.; Porter, D. F.; Thirsk, H. R. *J. Phys. Chem.* **1968**, *72*, 2300.
- (26) Wagner, C. D.; Riggs, W. M.; Davis, L. E.; Moulder, J. F.; Muilenberg, G. E. *Handbook of X-ray Photoelectron Spectroscopy*; Perkin Elmer: Eden Prairie, MN, 1979.
- (27) (a) de Silva, A. P.; Gunaratne, H. Q. N.; Gunnlaugsson, T.; Huxley, A. J. M.; McCoy, C. P.; Rademacher, J. T.; Rice, T. E. *Chem. Rev.* **1997**, *97*, 1515. (b) Lee, H.; Lee, H.-S.; Reibenspies, J. H.; Hancock, R. D. *Inorg. Chem.* **2012**, *51*, 10904.